# EPR Evidence for a Tyrosyl Radical Intermediate in Bovine Liver Catalase

Anabella Ivancich,† Hélène Marie Jouve,*,‡ and Jacques Gaillard†

*CEA-Grenoble, DRFMC, SCIB, Spectroscopie de Complexes Polymétalliques et de Métalloprotéines 17 Ave. des Martyrs, F-38054 Grenoble, France*
*Institut de Biologie Structurale Jean-Pierre Ebel CEA-CNRS, 41 Ave. des Martyrs, F-38027 Grenoble, France*

*Received August 13, 1996*

Catalases, like peroxidases, are enzymes responsible for the disproportionation of hydrogen peroxide into water and molecular oxygen.[1] The X-ray structure (2.5 Å) of bovine liver catalase (BLC) reveals that the active site consists of an iron−protoporphyrin IX prosthetic group with a tyrosinate axial ligand.[2] In native catalase, the heme site is in a high-spin ferric state, and the two-electron oxidation by hydrogen peroxide induces the formation of the so-called compound I, proposed to be an oxoferryl iron ($Fe^{4+}$═O) and a porphyrin $\pi$-cation radical ($por^{\bullet+}$). The first EPR evidence for compound I in catalases was recently reported for *Micrococcus luteus* (formerly *lysodeikticus*) catalase (MLC),[3] for which the observed EPR spectrum corresponds to a $por^{\bullet+}$ ($S = {}^1/_2$) having a ferromagnetic exchange interaction with the oxoferryl moiety ($S = 1$). In heme peroxidases, either porphyrin- or protein-based radical intermediates have been observed. For horseradish peroxidase (HRP) compound I, a $por^{\bullet+}$ was characterized by EPR and Mössbauer spectroscopies;[4] recently, a transient tyrosyl radical in equilibrium with $por^{\bullet+}$ was observed for the (Phe172 to Tyr) HRP mutant.[5] In compound I (or ES) of cytochrome *c* peroxidase (CcP) the organic radical originates from Trp191,[6] but in a mutant CcP (Trp191 to Phe) a tyrosyl radical EPR signal was reported.[7] Interestingly, the active site of ascorbate peroxidase shows structural homology to that of CcP but stabilizes a $por^{\bullet+}$ radical.[8]

In the present work, we report the EPR spectra of BLC treated with peroxyacetic acid[9] (Figure 1). In contrast to the *M. luteus* compound I,[3] the 9 GHz EPR spectrum of BLC (Figure 1A, top) shows at $g \approx 2$ a broad radical signal[11] (the overall breath is *ca.* 50 G) with hyperfine structure that resembles the $Tyr^{\bullet}_D$ and $Tyr^{\bullet}_Z$ from photosystem II (PSII).[12,13] The envelope of the 245 GHz EPR spectrum of BLC (Figure 1B, top) is dominated by *g*-anisotropy, with no well-resolved hyperfine pattern. The accurate g-values obtained from the simulated spectrum (Figure 1B, bottom) are 2.00777, 2.00460, and 2.00232 for $g_x$, $g_y$, and $g_z$, respectively.[14]

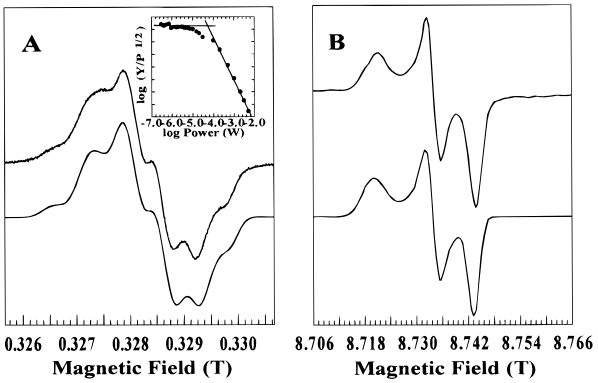


**Figure 1.** Experimental (top) and simulated (bottom) EPR spectra of the BLC radical. Parameters used for both simulations are those in Table 1. Both EPR spectra are obtained under nonsaturating conditions. Experimental conditions: (A) temperature, 86 K; microwave frequency, 9.222 GHz; modulation amplitude, 1.6 G; modulation frequency, 100 kHz; microwave power, 0.01 mW; (B) temperature, 10 K; microwave frequency, 244.996 GHz; modulation amplitude, 10 G (at 100 kHz); modulation frequency, 10 kHz. The X-band and high frequency spectrometers used were previously described.[35,36] Inset: power saturation curve obtained at 20 K; microwave frequency, 9.222 GHz; modulation amplitude, 1.6 G; modulation frequency, 100 kHz. The peak-to-peak height (*Y*) was measured as the maximum amplitude of the BLC radical signal in the X-band EPR spectrum.

Figure 1A (top) shows the experimental 9 GHz EPR spectrum of the BLC radical at 86 K. In order to estimate the hyperfine couplings contributing to this spectrum, we used a computer program[16] which calculates the powder EPR spectrum using as parameters the principal values of g and the hyperfine tensors, including its orientations with respect to the molecular axis.[14] On the basis of the similarities of the BLC radical and PSII $Tyr^{\bullet}$ EPR spectra, we used the experimental hyperfine coupling tensors of PSII $Tyr^{\bullet}$ [15,17] as the initial values for our simulations along with our experimentally determined *g*-values mentioned above. It has been shown that the observed differences in the EPR spectra of tyrosyl radicals from different enzymes arise from distinct hyperfine couplings of the $\beta$-methylene protons, while those of the α-protons at the phenol ring (C3, C5, C2, and C6) are almost invariant (see Table 1). Thus, in our simulations we fixed the parameters equivalent to the α-protons from the PSII $Tyr^{\bullet}$ and allowed progressive changes on those values equivalent to the hyperfine couplings of the $\beta$-methylene protons, until very reasonable agreement was achieved with the experimental spectrum of the BLC radical. A final fit varying all of the parameters was done with an iterative routine.[16] The resulting simulated spectrum in Figure 1A (bottom) was achieved by the set of parameter shown in Table 1. Comparison of these estimated parameters to those of tyrosyl radicals indicates that the spectral differences between the BLC radical and PSII $Tyr^{\bullet}$ can be accounted for by making very similar the isotropic (contact) part of the hyperfine interactions to the two

† CEA-Grenoble.
‡ Institut de Biologie Structurale Jean-Pierre Ebel.

(1) Deisseroth, A.; Dounce, A. L. *Physiol. Rev.* **1970**, *50*, 319−375.
(2) Fita, I.; Silva, A. M.; Murthy, M. R. N.; Rossmann, M. G. *Acta Crystallogr., Sect. B: Struct. Sci.* **1986**, *42*, 497−515.
(3) Benecky, M. J.; Frew, J. E.; Scowen, N.; Jones, P.; Hoffman, B. M. *Biochemistry* **1993**, *32*, 11929−11933.
(4) Shulz, C. E.; Devaney, P. W.; Winkler, H.; Debrunner, P. G.; Doan, N.; Chiang, R.; Rutter, R.; Hager, L. P. *FEBS Lett.* **1979**, *303*, 102−105
(5) Miller, V. P.; Goodin, D. B.; Friedman, A. E.; Hartmann, C.; Ortiz de Montellano, P. R. *J. Biol. Chem.* **1995**, *270*, 18413−18419.
(6) Sivaraja, M.; Goodin, D. B.; Smith, M.; Hoffman, B. M. *Science* **1989**, *245*, 738−740.
(7) Fishel, L. A.; Farnum, M. F.; Mauro, J. M.; Miller, M. A.; Kraut, J. *Biochemistry* **1991**, *30*, 1986−1996.
(8) Bonagura, C. A.; Sundaramoorthy, M.; Pappa, H. S.; Patterson, W. R.; Poulos, T. L. *Biochemistry* **1996**, *35*, 6107−6115.
(9) Samples of native BLC (hydrogen peroxide:hydrogen peroxide oxidoreductase, EC 1.11.1.6; Boehringer) dialyzed against 0.1 M Tris−HCl buffer, pH = 7.5 were mixed with a *ca.* 30-fold excess of peroxyacetic acid[10] at 0 °C and quickly frozen (15 s) in liquid nitrogen.
(10) Jones, P.; Middlemiss, D. N. *Biochem. J.* **1972**, *130*, 411−415.
(11) Spin quantification of the radical signal results in *ca.* 0.5 spins/heme.
(12) Babcock, G. T.; Barry, B. A.; Debus, R. J.; Hoganson, C. W.; Atamian, M.; McIntosh, L.; Sithole, I.; Yocum, C. F. *Biochemistry* **1989**, *28*, 9557−9565.
(13) For a review, see: Debus, R. J. *Biochim. Biophys. Acta* **1992**, *1102*, 269−352.
(14) An anisotropic line width ($W_x$ = 28.5 G, $W_y$ = 13.0 G, $W_z$ = 10.0 G) was used in the simulations. The largest component of the *g*-tensor was taken in the direction of the C1−C4−O axis of the tyrosine and the smallest component, perpendicular to the phenol ring (carbon numbers as in ref 15).
(15) Warncke, K.; Babcock, G. T.; McCracken, J. *J. Am. Chem. Soc.* **1994**, *116*, 7332−7340.
(16) Neese, F. Diploma Thesis, University of Konstanz, Germany, 1993.
(17) Tommos, C.; Tang, X.-S.; Warncke, K.; Hoganson, C. W.; Styring, S.; McCracken, J.; Diner, B.; Babcock, G. T. *J. Am. Chem. Soc.* **1995**, *117*, 10325−10335.

S0002-7863(96)02836-3 CCC: $12.00 

**Table 1.** Comparison of the *g* and Proton Hyperfine Coupling[j] Tensors of the BLC Radical with Those of Tyrosyl Radicals from RNR and PSII

| | RNR $Tyr^{\bullet}$[a] | RNR $Tyr^{\bullet}$[b] | PSII $Tyr^{\bullet}_D$[c] | PSII $Try^{\bullet}_Z$[d] | BLC[i] |
|---|---|---|---|---|---|
| $g_x$ | 2.00912[e] | 2.00897 | 2.00740[f] | 2.00750[f] | 2.00777 |
| $g_y$ | 2.00457[e] | 2.00437 | 2.00425[f] | 2.00422[f] | 2.00460 |
| $g_z$ | 2.00225[e] | 2.00217 | 2.00205[f] | 2.00225[f] | 2.00232 |
| (3,5)$A_x$ | −26.7 | −32.2 | −25.4 | −26.8 | −25.9 |
| $A_y$ | −8.4 | −7.0 | −7.2 | −8.4 | −7.2 |
| $A_z$ | −19.6 | −19.9 | −19.5 | −19.5 | −19.5 |
| $\phi_{3,5}$ (deg) | ±25 | ±23 | ±23[g] | nd | ±23 |
| (2,6)$A_x$ | 5.0 | nd | 4.48[g] | 5.0 | 5.0 |
| $A_y$ | 7.6 | nd | 7.28[g] | 7.5 | 7.4 |
| $A_z$ | 2.1 | nd | 4.48[g] | 1.3 | <3.0 |
| $\phi_{2,6}$ (deg) | ±44 | nd | ±10[g] | nd | ±10 |
| $\beta_1$ $A_x$ | 61.2 | 20.72 | 29.3 | 35.4 | 20.0 |
| $A_y$ | 53.7 | 29.40 | 20.2 | 28.5 | 15.5 |
| $A_z$ | 53.7 | 26.60 | 20.2 | 29.2 | 16.0 |
| $A_{iso}$ | 56.2 | 25.6 | 23.2 | 31.0 | 17.2 |
| $\theta_1$ (deg) | 30[h] | −5 to 51 | 52 | 44 | 57 |
| $\beta_2$ $A_x$ | 2.1 | <8.4 | 14.3 | 7.9 | 14.5 |
| $A_y$ | −5.0 | <8.4 | 5.2 | 1.0 | 11.9 |
| $A_z$ | −4.0 | <8.4 | 5.2 | 1.7 | 10.6 |
| $A_{iso}$ | −2.3 | <8.4 | 8.2 | 3.5 | 12.3 |
| $\theta_2$ (deg) | 90[h] | nd | 68 | 76 | 63 |

[a] *Escherichia coli* RNR.[31] [b] *Salmonella typhimurium* RNR.[25] [c] *Synechocystis* PSII (WT).[15] [d] D2-YF(160) mutant of *Synechocystis* PSII.[17] [e] From ref 32. [f] From ref 27. [g] From ref 33. [h] From ref 34. [i] This work. An isotropic line width of 2.0 G was used for the X-band spectral simulations. For the α-protons, the *y*-axis is defined in the direction of the $C_n-H_n$ ($n$ = 2,3,5,6) bonds and the *z*-axis is perpendicular to the plane of the ring; the angle $\phi$ reflects the noncoincidence with the *g*-tensor axis.[15] The axis for the $\beta$-protons were taken coincident with the *g*-axes, $\theta$ being the dihedral angle defined in ref 19. Our experimental *g*-values are reproducible within $3 \times 10^{-5}$. [j] In MHz.

$\beta$-methylene protons in PSII ($A_{iso}$[18] of *ca.* 17 MHz and 12 MHz for $\beta_1$ and $\beta_2$, respectively). From geometrical considerations,[18] the resulting dihedral angles ($\theta_{1,2}$) would be 57° and 63°, which imply a more symmetrical location of the $\beta$-protons for BLC (see Table 1). These results, together with the fact that the reported hyperfine couplings of the few other well-characterized protein-based radicals, such as glycyl and lysyl radicals, observed in pyruvate formate lyase[21] and lysine 2,3-aminomutase,[22] respectively, are not suitable to simulate the BLC EPR spectrum,[23] suggest that the observed BLC radical originates from a tyrosine residue.

The 245 GHz EPR spectra of different tyrosyl radicals[24,25] showed significative differences for the $g_x$-values; a correlation between such $g_x$-values and the hydrogen bond pattern of the phenol oxygen was deduced by molecular orbital calculations.[24] Accordingly, the $g_x$-value obtained for the BLC radical (2.00777) strongly argues for the phenol oxygen being weakly H-bonded. It was also proposed that the amplitude distortion observed in the high-frequency (WT) PSII $Tyr^{\bullet}_D$ spectra was due to the influence of a paramagnetic relaxer (the Mn cluster or the non-heme high-spin $Fe^{2+}$) on the spin of the radical, and thus, a geometric term to account for anisotropic dipolar relaxation effects was used in the simulations.[26] In addition, a broadness on the $g_x$-edge of the spectrum of the $Tyr^{\bullet}_Z$ mutant as compared to that of the WT PSII $Tyr^{\bullet}_D$ was attributed to a distribution in $g_x$-values.[27] In contrast, the RNR[24,25] high-frequency spectrum could be readily simulated with an isotropic line width of 21.4 G.[25] Interestingly, the requirement of an anisotropic line width[14] for simulating the 245 GHz EPR spectrum of BLC (Figure 1B) argues for a $g_x$-distribution effect as in the mutant PSII radical. Nevertheless, the power saturation curve (Figure 1A, inset) that yields a $P_{1/2} = 0.060$ mW at 20 K indicates that the BLC radical is relaxed by the oxoferryl iron from the heme active site. In order to assess the influence of this interaction on the 245 GHz spectrum of BLC, further experimental data would be required.

In conclusion, we propose that the unprecedented radical species we detected in BLC (treated with peroxyacetic acid) originates from a protein amino acid residue, most probably a tyrosine. This radical should be formed either (i) as the second oxidizing equivalent in compound I, instead of the porphyrin radical observed in *M. luteus* catalase or most likely (ii) when reducing the porphyrin radical of compound I. In fact, resonance Raman studies on BLC showing a predominantly $^2A_{2u}$ $\pi$-cation radical character for the compound I[28] strongly argue against the first possibility (i). Interestingly, a tyrosyl radical has been theoretically proposed in the catalytic scheme of BLC which involves the enzyme-bound NADPH with a protective role.[29] Under this scheme, NADPH first reacts readily with a hypothetical intermediate state [$(Fe^{4+}{=}O)Tyr^{\bullet}$] formed by spontaneous decay of compound I [$(Fe^{4+}{=}O)por^{\bullet+}$], before it finally restores the enzyme to the native state ($Fe^{3+}$).[29,30] Further studies are in progress in our laboratories, including site-directed mutagenesis in related bacterial catalases, to confirm our proposal and identify the tyrosine residue responsible for the radical formation in bovine liver catalase.

**Acknowledgment.** We thank E. Girard for his help with the simulations, Dr. A.-L. Barra for her assistance during HF measurements, and the High Magnetic Field Laboratory (CNRS) for providing facilities. We thank Drs. M. Atta, B. Lamotte, T. A. Mattioli, and J. M. Mouesca for stimulating discussions. A.I. acknowledges a C. T. E. contract from CEA and a fellowship from CONICET (Argentina).

JA9628361

(18) The $A_{iso}$ for the $\beta$-protons was calculated from the tensor components in Table 1. The angle dependent McConnell relation[19] $A_{iso} \approx B_2\, \rho_{C1} \cos^2 \theta$ was used ($B_2 = 162$ MHz[20]), together with the restriction $/\theta_1 + \theta_2/ = 120°$, where $\theta$ is the dihedral angle between the $C_\beta-H_\beta$ bond and the normal to the tyrosine ring[15] and $\rho_{C1}$ is the spin density distribution on $C_1$.

(19) Stone, E. W.; Maki, A. H. *J. Chem. Phys.* **1962**, *37*, 1326−1333.
(20) Fessender, R. W.; Schuler, R. H. *J. Chem. Phys.* **1963**, *39*, 2147−2195.
(21) Wagner, A. F. V.; Frey, M.; Neugebauer, F. A.; Schäfer, W.; Knappe, J. *Proc. Natl. Acad. Sci. U.S.A.* **1992**, *89*, 996−1000.
(22) Ballinger, M. D.; Frey, P. A.; Reed, G. H. *Biochemistry* **1992**, *31*, 10782−10789.
(23) The possibility that hyperfine couplings of a "tyrosine-like" radical might yield a similar EPR spectrum cannot be formally excluded.
(24) Un, S.; Atta, M.; Fontecave, M.; Rutherford, A. W. *J. Am. Chem. Soc.* **1995**, *117*, 10713−10719.
(25) Allard, P.; Barra, A. L.; Andersson, K. K.; Schmidt, P. P.; Atta, M.; Gräslund, A. *J. Am. Chem. Soc.* **1996**, *118*, 895−896.
(26) Un, S.; Brunel, L.-C.; Brill, T. M.; Zimmermann, J.-L.; Rutherford, A. W. *Proc. Natl. Acad. Sci. U.S.A.* **1994**, *91*, 5262−5266.
(27) Un, S.; Tang, X-S; Diner, B. A. *Biochemistry* **1996**, *35*, 679−684.
(28) Chuang, W.-J.; Van Wart, H. E. *J. Biol. Chem.* **1992**, *267*, 13293−13301.
(29) Hillar, A.; Nicholls, P.; Switala, J.; Loewen, P. C. *Biochem. J.* **1994**, *300*, 531−539.
(30) Olson, L. P.; Bruice, T. C. *Biochemistry* **1995**, *34*, 7335−7347.
(31) Hoganson, C. W.; Sahlin, M.; Sjöberg, B.-M.; Babcock, G. T. *J. Am. Chem. Soc.* **1996**, *118*, 4672−4679.
(32) Gerfen, G. J.; Bellew, B. F.; Un, S.; Bollinger, J. M.; Stubbe, J.; Griffin, R. G.; Singel, D. J. *J. Am. Chem. Soc.* **1993**, *115*, 6420−6421.
(33) Tommos, C.; Madsen, C.; Styring, S.; Vermaas, W. *Biochemistry* **1994**, *33*, 11805−11813.
(34) Bender, C. J.; Sahlin, M.; Babcock, G. T.; Barry, B. A.; Chandrasekar, T. K.; Salowe, S. P.; Stubbe, J.; Lindström, B.; Petersson, L.; Ehrenberg, A.; Sjöberg, B.-M. *J. Am. Chem. Soc.* **1989**, *111*, 8076−8083.
(35) Schoepp, B.; Parot, P.; Menin, L.; Gaillard, J.; Richaud, P.; Verméglio, A. *Biochemistry* **1995**, *34*, 11736−11742.
(36) Muller, F.; Hopkins, M. A.; Coron, N.; Grynberg, M.; Brunel, L. C.; Martinez, G. *Rev. Sci. Instrum.* **1989**, *60*, 3681−3684.